Embelin Suppresses Dendritic Cell Functions and Limits Autoimmune Encephalomyelitis Through the TGF-β/β-catenin and STAT3 Signaling Pathways

**Zhenyi Xue · Zhenzhen Ge · Kai Zhang · Rui Sun ·
Juhong Yang · Rong Han · Meiyu Peng · Yan Li · Wen Li ·
Da Zhang · Junwei Hao · Yurong Da · Zhi Yao · Rongxin Zhang**

Abstract Embelin (2,5-dihydroxy-3-undecyl-1,4-benzoquinone, EB) has been shown to inhibit the X-linked inhibitor of apoptosis protein and various inflammatory pathways. Although different molecular mechanisms have been described for the potent antitumor activities of EB, its potential effect on inflammatory and immune-mediated diseases such as multiple sclerosis (MS) and its animal model experimental autoimmune encephalomyelitis (EAE) remains unclear. In this study, we demonstrated that EB suppressed human CD14$^+$ monocyte-derived dendritic cell (DC) differentiation, maturation, and endocytosis and further inhibited the stimulatory function of mature DCs on allogeneic T cell proliferation in vitro. In addition, EB blocked the DC-derived expression of the Th1 cell-polarizing cytokines interferon-γ and interleukin (IL)-12 and the Th17 cell-polarizing cytokines IL-6 and IL-23. In vivo administration of EB led to a reduction in the EAE clinical score, in central nervous system inflammation, and in demyelination. Furthermore, EB also suppressed inflammatory Th1 and Th17 cells in EAE, at least partially, through the promotion of transforming growth factor-beta and β-catenin expression and inhibition of signal transducer and activator of transcription 3 signaling pathways in DCs. These data suggest that EB has potent anti-inflammatory and immunosuppressive properties and is a potential therapeutic drug for MS and other autoimmune inflammatory diseases.

Zhenyi Xue, Zhenzhen Ge, and Kai Zhang contributed equally to this work.

Z. Xue · Z. Ge · K. Zhang · R. Sun · R. Han · M. Peng · Y. Li ·
W. Li · Y. Da · R. Zhang
Laboratory of Immunology and Inflammation, Research Center of
Basic Medical Science, Tianjin Medical University, Tianjin 300070,
China

Z. Xue · Z. Ge · K. Zhang · M. Peng · Y. Li · W. Li · Y. Da ·
Z. Yao (✉) · R. Zhang
Department of Immunology, Basic Medical College, Tianjin Medical
University, Tianjin 300070, China
e-mail: yaozhi@tijmu.edu.cn

Z. Xue · Z. Ge · K. Zhang · M. Peng · Y. Li · W. Li · Y. Da · Z. Yao ·
R. Zhang
Tianjin Key Laboratory of Cellular and Molecular Immunology,
Tianjin Medical University, Tianjin 300070, China

Z. Xue · Z. Ge · K. Zhang · M. Peng · Y. Li · W. Li · Y. Da · Z. Yao ·
R. Zhang
Key Laboratory of Immune Microenvironment and Diseases of
Educational Ministry of China, Tianjin Medical University,
Tianjin 300070, China

J. Yang
Tianjin Metabolic Diseases Hospital, Tianjin Medical University,
Tianjin 300070, China

D. Zhang
School of Medical Imaging, Tianjin Medical University,
Tianjin 300070, China

J. Hao
Department of Neurology, Tianjin Neurological Institute, Tianjin
Medical University General Hospital, Tianjin 300052, China

R. Zhang (✉)
Center for Basic Medical Science Research, Tianjin Medical
University, Tianjin 300070, China
e-mail: rongxinz@yahoo.com

Abbreviations
EB   Embelin
MS   Multiple sclerosis
EAE   Experimental autoimmune encephalomyelitis
iDC   Immature dendritic cell
mDC   Mature dendritic cell

Introduction

Embelia ribes Burm (Myrsinaceae), an herbaceous medicinal plant, has been traditionally used to treat fever, dyspepsia, various gastrointestinal ailments, and skin disease [1]. Embelin (EB), an active compound from this plant, has shown significant antiproliferative and pro-apoptotic effects on cells in fibrosarcoma [2], leukemia [3–5], pancreatic cancer [6, 7], breast cancer [8], colon cancer [9], multiple myeloma [10], and prostate cancer [11]. Other reports have clearly demonstrated that EB is a potent inhibitor of the activation of pro-inflammatory transcription factors, such as nuclear factor-kappaB [4] and signal transducer and activator of transcription 3 (STAT3) [10]. Additionally, EB has also been reported to induce apoptosis through the upregulation of peroxisome proliferator-activated receptor-gamma (PPARγ) transcription [9], the targeting of microtubular proteins [12], and the cleavage of receptor-interacting protein [6] in addition to significantly increasing PPARγ expression in type 2 diabetic rats [13]. Recently, EB was found to inhibit growth and induce apoptosis through the suppression of Akt/mTOR/S6K1 signaling cascades [14]. Although various molecular mechanisms, as discussed previously, have been suggested to account for the potent antitumor activities of EB, its potential effect on multiple sclerosis (MS) and its animal model experimental autoimmune encephalomyelitis (EAE) remains unclear.

Dendritic cells (DCs) have a pivotal role in the immune response and in stimulating naïve T lymphocytes [15]. DCs also have a critical role in the induction and maintenance of self-tolerance, the failure of which can lead to autoimmune/inflammatory diseases. Recent evidence suggests that DCs are critical for the suppression of immune responses through the generation of T regulatory cells (Treg cells) [16, 17]. How DCs accomplish these seemingly contradictory functions in immunity vs. tolerance is unclear. The general features of DC maturation are well understood [18] and involve the translocation of major histocompatibility complex class II molecules (MHC-II), the upregulation of co-stimulatory molecules such as CD80 and CD86, the activation of lysosomal antigen processing, and the release of a host of immunostimulatory cytokines [19]. Such cytokines regulate the differentiation of naïve CD4$^+$ T cells into either inflammatory cells [T helper 1 (Th1), Th2, or Th17] or Treg cells, thereby regulating the balance between immunity and tolerance. In both MS and EAE, Th1 and Th17 myelin-reactive CD4$^+$ T lymphocytes gain access to the central nervous system (CNS) and, in concert with other infiltrating mononuclear cells such as macrophages, cause inflammation, oligodendrocyte cell death, demyelination, axonal degeneration, and progressive ascending paralysis [20–22]. However, Th2 mediated the suppression of autoimmune disease [23].

EAE is an autoimmune disorder of the CNS that serves as an animal model for human MS [24]. A strong body of evidence points to a role for transforming growth factor-beta (TGF-β) in preventing EAE [25–32]. A recent study found that TGF-β signaling in DCs is a prerequisite for the control of autoimmune encephalomyelitis [33]. Although these observations demonstrate a critical protective function for TGF-β in EAE, the targets of TGF-β activity remain undefined.

Recent data from in vitro and in vivo experiments point to a critical role for β-catenin signaling in the regulation of DC [34] and Treg cell function [35]. β-Catenin is involved in many complex interactions and has many functions [36]. β-Catenin is an essential component of the Wnt signaling (Wnts) pathway, which controls a number of processes linked to embryonic and organ development [37]. The absence of Wnts facilitates the phosphorylation of β-catenin protein by glycogen synthase kinase-3 beta (GSK-3β), leading to β-catenin ubiquitination and degradation [38], whereas Wnts can induce the phosphorylation and inactivation of GSK-3β and promote the subsequent stabilization of β-catenin protein [39]. Moreover, TGF-β suppresses the β-catenin-dependent tolerogenic activation program in DCs [40]. DCs induce tolerance in vivo, and more importantly, immunization with DCs can provide complete protection against autoimmune diseases such as EAE.

A number of immunomodulatory drugs, including β-interferon (Avonex, Betaseron, and Rebif), glatiramer acetate (Copaxone), mitoxantrone (Novantrone), natalizumab (Tysabri), and fingolimod (Gilenya), have been introduced as a treatment for MS. There are several drugs undergoing phase II and III trials. However, current drugs have been proven unsatisfactory because of their toxicity in a number of patients [41]. Therefore, the improvement of MS therapy through the development of new drugs is necessary.

In this study, we investigated whether EB affects DC differentiation and activation by monitoring DC cytokine production and mature DC (mDC) allostimulatory activity during the T cell proliferation process that ameliorates EAE. In conclusion, EB significantly increased TGF-β/β-catenin signaling and decreased STAT3 phosphorylation in DCs, by reducing the levels of various pro-inflammatory factors. This

led to a reduction of EAE clinical score and CNS inflammation and demyelination. This study also provided further insights into the biological functions and clinical applications of EB and demonstrated the need for further investigation of EB as a potential therapeutic drug for MS and other autoimmune inflammatory diseases.

Materials and Methods

Animals

Female C57BL/6 mice aged 6–8 weeks were purchased from the Academy of Military Medical Science (Beijing, China). The animals were housed and fed in a specific pathogen-free animal facility at the Experimental Animal Center of Tianjin Medical University (Tianjin, China). The experiments were performed in accordance with the guidelines for animal care and were approved by the Animal Ethics Committee of Tianjin Medical University (Tianjin, China).

CD14$^+$ Cell Purification and DC Differentiation and Maturation

Fresh human buffy coats were obtained from the Tianjin Blood Center (Tianjin, China). Peripheral blood mononuclear cells (PBMCs) were isolated by centrifugation through Ficoll-Paque PLUS (Amersham Biosciences, Uppsala, Sweden) at $400 \times g$ for 30 min, and the upper layer (plasma) was drawn off using a sterile Pasteur pipette, leaving the lymphocyte layer undisturbed at the interface. Using a clean sterile Pasteur pipette, the lymphocyte layer was transferred to a clean centrifuge tube and then washed three times with phosphate-buffered saline (PBS). The CD14$^+$ monocytes were separated from the PBMCs using a magnetic separation column in accordance with the manufacturer's instructions (Miltenyi Biotech, Auburn, CA, USA) and were washed thoroughly to eliminate the unspecific binding of cells to the beads. The purified CD14$^+$ monocytes were analyzed on a FACSCalibur instrument (Becton Dickinson, San Jose, CA, USA) to confirm the purity of the CD14$^+$ cells (>95 %). Complete Roswell Park Memorial Institute (RPMI) 1640 culture medium containing 100 mM sodium pyruvate, 200 mM L-glutamine, 100 mg/ml kanamycin, and 10 % fetal bovine serum (FBS) (Gibco, Invitrogen Auckland, New Zealand) was used for the routine culture of the primary cells. For DC differentiation, the purified CD14$^+$ cells were cultured for 5 days in the presence of 1,000 U/ml recombinant human granulocyte–macrophage colony-stimulating factor (GM-CSF) and 1,000 U/ml interleukin-4 (IL-4) (Peprotech, Rocky Hill, NJ, USA) and were simultaneously treated either with or without 10, 30, or 60 µM EB (Haoyuan Chemexpress Co., Ltd., Shanghai, China). To induce DC maturation, the immature DCs (iDCs) with or without EB treatment were treated with 1 µg/ml lipopolysaccharide (LPS; Sigma, St. Louis, MO, USA) on day 5 and were incubated for an additional 2 days in complete RPMI 1640 medium.

Flow Cytometry Analysis

Cells were harvested on day 5 for the analysis of human CD14$^+$ monocyte-derived DC differentiation or on day 7 for the analysis of maturation. The DCs were stained for the surface markers CD80, CD83, CD86, and HLA-DR using antihuman, fluorescence-conjugated antibodies and were stained simultaneously with phycoerythrin (PE)-conjugated CD11c antibody (BD Biosciences, San Jose, CA, USA). A fluorescence-activated cell sorter (FACS) was used for the analysis. The FACS data were analyzed using FlowJo software (Tree Star, Ashland, OR, USA).

Endocytosis Analysis of iDCs

Endocytosis was quantified as the cellular uptake of fluorescein isothiocyanate (FITC)–dextran (MW, 40,000; Sigma, St. Louis, MO, USA). iDCs were incubated in medium containing FITC–dextran (0.1 mg/ml) and were treated with or without EB at either 4 °C as the negative control or at 37 °C as the positive control for 30 min. The cells were washed and were analyzed on a FACSCalibur as described previously.

Mixed Lymphocyte Reaction (MLR) Assay

The CD4$^+$ T cells were positively selected from fresh PBMCs using antihuman CD4-conjugated microbeads (Miltenyi Biotec, Auburn, CA, USA). The purified CD4$^+$ T cells were resuspended in PBS (10^7 cells/ml) and treated with 2 µM carboxyfluorescein succinimidyl ester (CFSE; marker for cell proliferation; Invitrogen, Eugene, OR, USA) for 30 min at 37 °C. The cells were then washed twice with complete RPMI 1640 medium to terminate the staining process. The LPS-activated mDCs with or without EB treatment were pretreated using mitomycin C (proliferation blocker, 25 µg/ml) before being cocultured with the CD4$^+$ T cells. The CFSE-labeled CD4$^+$ cells and the pretreated DCs were added to each well of a U-bottom microtiter plate (2×10^5 cells/well). The mDCs were cocultured with the allogeneic CD4$^+$ T cells at ratios of 1:10, 1:20, and 1:40 for 4 days. The cells were acquired using a FACSCalibur instrument (Becton Dickinson, San Jose, CA, USA), and the data were analyzed using the FlowJo software. The results, represented by the proliferation index (PI), were calculated by ModFit. The PI is the sum of the cells in all generations divided by the calculated number of original parent cells.

Quantitative Real-Time Polymerase Chain Reaction (PCR)

RNA was extracted using TRIzol reagent (Invitrogen, Carlsbad, CA, USA) in accordance with the manufacturer's instructions. After RNA purification, the samples were treated with DNase to remove the contaminating genomic DNA. Reverse transcription was performed using random hexamers and M-MLV reverse transcriptase (Promega, Madison, WI, USA). All other reverse transcription reagents were supplied by Takara (Takara, Japan). The gene-specific primers were synthesized at BGI (Beijing, China). For relative quantitative real-time PCR, SYBR Green mix (Takara, Japan) was used in accordance with the manufacturer's instructions. The reactions were performed in triplicate on an ABI PRISM 7500 Fast Real-Time PCR System (Applied Biosystems Inc., Foster City, CA, USA), and the generated products were analyzed using ABI 7500 software (version 2.0.5; Applied Biosystems Inc., Foster City, CA, USA). The primer pairs are listed as follows:

Human gene primers	Sense (5′–3′)	Antisense (5′–3′)
IL-23p19	GGACAACAGTCAGTTCTGCTT	CACAGGGCTATCAGGGAGC
IL-12p40	ACAAAGGAGGCGAGGTTCTAA	CCCTTGGGGGTCAGAAGAG
IL-12p35	CCTTGCACTTCTGAAGAGATTGA	ACAGGGCCATCATAAAAGAGGT
IL-6	AAATTCGGTACATCCTCGACGG	GGAAGGTTCAGGTTGTTTTCTGC
TNF-α	GAGGCCAAGCCCTGGTATG	CGGGCCGATTGATCTCAGC
IFN-γ	CTCTTGGCTGTTACTGCCAGG	CTCCACACTCTTTTGGATGCT
GAPDH	ACCACAGTCCATGCCATCAC	TCCACCACCCTGTTGCTGTA

Gene expression values were normalized based on the GAPDH mRNA levels. GAPDH mRNA remains at constant levels in the experimental conditions and additional housekeeping genes 18S were tested, the results are unanimous (data not shown). Data are presented as the $2^{-\Delta\Delta Ct}$ values and are representative of at least three independent experiments.

Western Blot Analysis

DCs were lysed in buffer containing 10 mM Tris buffer (pH 7.6), 1 % Triton X-100, 1 % phosphatase inhibitor cocktail, and 1 mM PMSF. The lysates were boiled in sodium dodecyl sulfate (SDS) sample buffer and were subjected to SDS-PAGE. Rabbit monoclonal antibodies against GAPDH, TGF-β, phosphorylated STAT3 (phosphorylated on residue Tyr705), and phosphorylated glycogen synthase kinase-3 beta

(p-GSK-3β, phosphorylated residue Ser-9) were purchased from Cell Signaling Technology (Beverly, MA, USA) and were diluted 1:1,000. Rabbit monoclonal antibodies against β-catenin were purchased from Abcam (Eugene, OR, USA) and were diluted 1:1,000. Horseradish peroxidase-conjugated goat anti-rabbit immunoglobulin G (Santa Cruz Biotechnology, Santa Cruz, CA, USA) was used as the secondary antibody. Immunoreactive bands were identified using the ECL Western Blotting Detection System (Millipore Corporation, Billerica, MA, USA).

Induction and Treatment of EAE

For EAE induction, the C57BL/6 mice (aged 6–8 weeks) were immunized (s.c.) with 150 mg of myelin oligodendrocyte glycoprotein (MOG residues 35–55). The peptide sequence was Met-Glu-Val-Gly-Trp-Tyr-Arg-Ser-Pro-Phe-Ser-Arg-Val-Val-His-Leu-Tyr-Arg-Asn-Gly-Lys and the purity was >95 % (CL Bio-Scientific Co., Ltd., Xi'an, China). The immunization was performed by mixing the MOG$_{35-55}$ peptide with complete Freund's adjuvant containing 5 mg/ml of heat-killed H37Ra, a *Mycobacterium tuberculosis* strain (Difco Laboratories, Detroit, MI, USA). Pertussis toxin (400 ng) (List Biological Laboratories, Campbell, CA, USA) in PBS and 50 mM NaCl was administered i.p. on the day of immunization and again after 24 h. For the treatment of EAE, EB (25 and 50 mg/kg) or PBS (vehicle control) was administered p.o. daily started at days of immunization. The mice were weighed and examined daily for disease symptoms, which were assessed using the following standard score system: 0, no obvious changes in motor functions; 1.0, limp tail; 2.0, limp tail and wobbly gait; 3.0, bilateral hind limb paralysis; 4.0, complete hind limb and partial forelimb paralysis; and 5.0, death [42].

DC Response Ex Vivo

For the ex vivo study, samples of splenocytes isolated from EAE mice on day 7 were cultured in triplicate at a density of 5×10^5 cells/well in 96-well plates containing complete RPMI 1640 medium and the MOG peptide (20 μg/ml). EB at the indicated concentrations or the PBS vehicle was added to the culture as appropriate. The cultures were maintained at 37 °C in 5 % CO$_2$ for 72 h. For surface staining, the splenocytes from either EB-treated or PBS-treated mice were restimulated with the MOG peptide (20 μg/ml) for 48 h. The expression of CD11c, CD80, CD86, and MHC-II (Sungene, Tianjin, China) were analyzed by staining the cells ($0.5-1\times10^6$) with fluorochrome-conjugated specific mAbs or isotype controls (BD Pharmingen, Franklin Lakes, NJ, USA) diluted in PBS containing 1 % BSA in accordance with the manufacturer's protocol.

Histopathology and Immunohistochemistry

The spinal cords from mice transcardially perfused with 4 % paraformaldehyde were dissected and postfixed overnight. The paraffin-embedded 5–10 µm spinal cord sections were stained with hematoxylin and eosin (H&E) for routine histological analysis of inflammatory infiltration and with Luxol fast blue (Alfa Aesar, Ward Hill, MA, USA) for the evaluation of demyelination. For immunohistochemical evaluation, the paraffin sections were immunostained with anti-F4/80 (AbD Serotec, Oxford, UK) to evaluate macrophage infiltration according to the IHC WORLD Protocol Database.

Intracellular Cytokine Staining

A single cell suspension was isolated from the spleens of PBS-treated or EB-treated EAE mice on day 14 by mashing the tissue and passing it through a 40-µm nylon cell strainer (BD Biosciences, San Jose, CA, USA). Next, the cells were restimulated with 1 µg/ml brefeldin A (Sigma, St. Louis, MO, USA), 600 ng/ml phorbol 12-myristate 13-acetate (PMA; Enzo Life Sciences, Farmingdale, NY, USA) and 1 µg/ml ionomycin (Enzo Life Sciences, Farmingdale, NY, USA) for 5 h in complete RPMI 1640 culture medium containing 100 mM sodium pyruvate, 200 mM L-glutamine, 100 mg/ml kanamycin, and 10 % FBS and were collected and washed with PBS. To stain for a cell surface marker, the APC-conjugated rat anti-mouse CD4 antibody (eBioscience, San Diego, CA, USA) was used. The cells were fixed and permeabilized and then stained for intracellular cytokines using PE-conjugated rat anti-mouse IL-17 or FITC-conjugated rat anti-mouse interferon-γ (IFN-γ; eBioscience, San Diego, CA, USA). Nonspecific staining was monitored using isotype antibody controls. The cells were analyzed by FACSCalibur, and the acquired data were analyzed using the FlowJo software and WinMDI 2.9 software.

Isolation of Mononuclear Cells that Infiltrate the CNS during EAE

Mice were anesthetized and perfused through the left ventricle with ice-cold 1× Hank's balanced salt solution (HBSS). The dissected brain and spinal cord were maintained in RPMI without phenol red until all of the mice are sacrificed. The tissues were placed in a Dounce homogenizer containing RPMI, and a pestle was used to gently dissociate the tissues and make a cell suspension. The cell suspensions were separated over discontinuous 70 %/30 % Percoll gradients and centrifuged for 30 min at 500×g and 18 °C. Using a transfer pipette, the layer of debris was gently removed from the top of the tube, and 2.0–3.0 ml of the 70 %/30 % interphase was transferred to a clean conical tube containing 1× HBSS. Percoll containing the interphase was diluted approximately

threefold, mixed repeatedly by inversion, and centrifuged for 7 min at 500×g and 18 °C. The pellet was then resuspended in 1 ml PBS buffer for subsequent analysis.

Statistical Analysis

The experiments were performed in triplicate on three separate occasions. One-way analysis of variance, where applicable, was performed to determine whether an overall statistically significant change existed before the Student's t test was used to analyze the difference between any two groups. $p < 0.05$ was considered statistically significant. In addition, the standard deviations (SDs) from the mean, expressed as the SD values or as equivalent error bars, were calculated.

Results

EB Inhibits the Differentiation and Endocytosis of Human Monocyte-Derived DCs

To determine the effects of EB on the differentiation of monocyte-derived DCs, purified CD14$^+$ monocytes were allowed to differentiate into iDCs in the presence of various concentrations of EB (10, 30, and 60 µM), GM-CSF, and IL-4. After 5 days of culture, changes in the expression level of the co-stimulatory molecules CD80, CD86, CD83, and HLA-DR were assessed using flow cytometry. Compared with the day 5 untreated iDCs, a significant dose-dependent reduction in cell surface marker expression was observed in EB-treated cells, as was demonstrated by the mean fluorescence intensity (MFI) histograms (Fig. 1a) and the relative MFI levels in EB-treated cells and PBS-treated controls (Fig. 1b). These results indicate that EB inhibited the differentiation of human CD14$^+$ monocytes into DCs in a dose-dependent manner.

To further investigate whether EB affected the antigen uptake capacity of iDCs, we examined the endocytosis function of iDCs by estimating the uptake of FITC–dextran. As shown in Fig. 1c, FITC–dextran uptake decreased gradually in EB-treated iDCs in a dose-dependent manner compared with the PBS-treated iDC. The maximum inhibition of FITC–dextran uptake in iDCs was observed following treatment with 30 µM EB, and this was similar to the uptake observed in the negative control (iDCs at 4 °C). These data suggest that EB impaired the endocytosis function of iDCs.

EB Suppresses Both the Maturation of iDCs and mDC-Induced Allogeneic T Cell Proliferation

mDCs functionally present antigens to T cells and initiate immune responses. Therefore, it was critical to determine the effect of EB on the phenotypic maturation of DCs. iDCs, with or without EB treatment, were activated by the addition

a

b

c
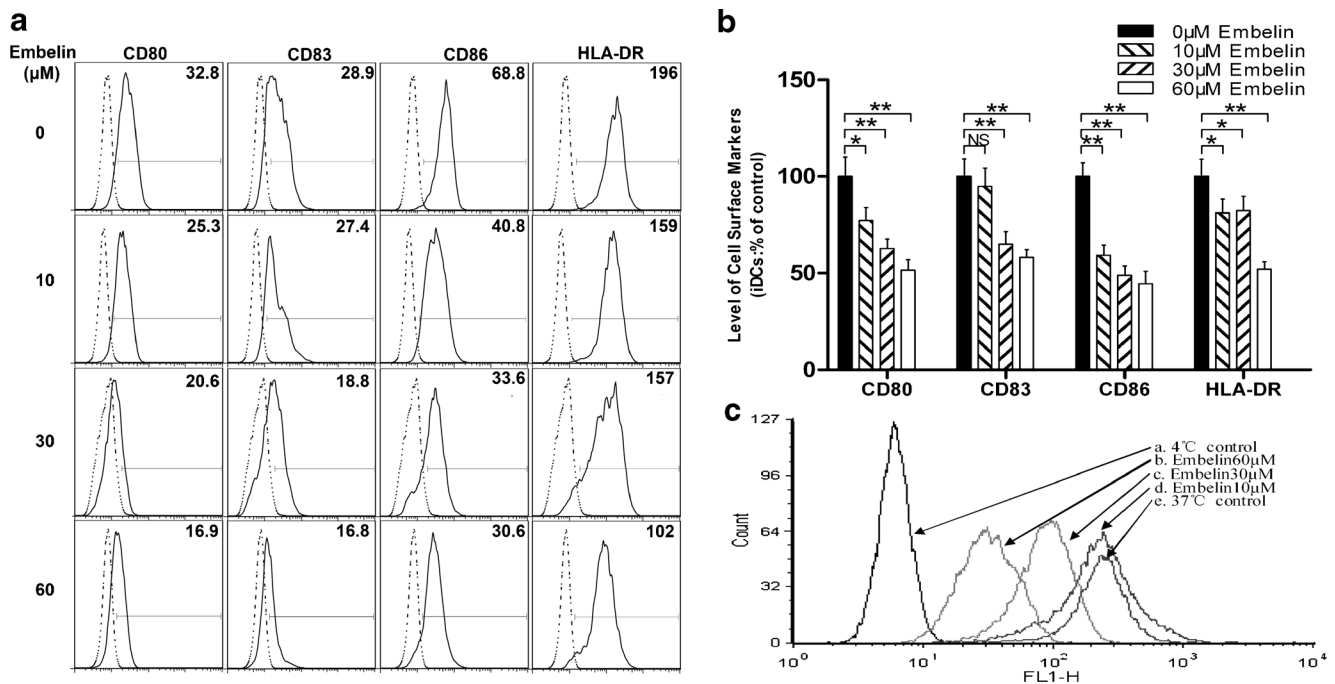
Fig. 1 EB inhibited the differentiation and endocytosis of monocyte-derived DCs. The indicated doses of EB were added on day 0 and were replenished on day 3 during the differentiation of the $CD14^+$ monocytes to DCs by GM-CSF an IL-4. The cell surface markers CD80, CD83, CD86, and HLA-DR were examined on day 5 by FACS analysis. FITC-conjugated antibodies against these marker molecules were used for staining. **a** Histograms of the cell surface marker staining from one of three independent experiments. The *numbers* indicate the MFI of the stained cells. **b** Relative levels of cell markers compared with the EB-untreated controls (100 %) from three independent experiments with means±SD. NS>0.05, *$p<0.05$, **$p<0.01$ determined by Student's t

test. **c** The FITC–dextran uptake by iDCs was evaluated by flow cytometry after 30 min of incubation with FITC–dextran at either 37 or 4 °C. *a* Control: EB-untreated iDCs incubated with FITC–dextran at 4 °C for 30 min (negative control). *b*, *c*, and *d* iDCs treated with 60, 30, and 10 μM EB, respectively, and incubated with FITC–dextran at 37 °C for 30 min. *e* 37 °C control: EB-untreated iDCs incubated with FITC–dextran at 37 °C for 30 min (positive control). *x*-axis represents the FITC-labeled dextran antigen, *y*-axis represents the endocytosis cell counts. The data are representative of three independent experiments using different blood donors

of 1 μg/ml LPS for 2 days, and the expression of the mDC surface markers CD80, CD83, CD86, and HLA-DR was determined using flow cytometry. As shown in Fig. 2a, control mDCs demonstrated a significant increase in CD80, CD83, CD86, and HLA-DR expression following LPS activation. However, mDCs treated with EB (10, 30, and 60 μM) demonstrated a gradual reduction in the expression levels of CD80, CD83, and CD86 compared with control mDCs (Fig. 2b). These results indicated that EB inhibited LPS-induced DC maturation.

To investigate whether EB impaired mDC-mediated allogeneic T cell activation and proliferation, allogeneic T cell proliferation stimulated by mDCs either treated or untreated with EB was assessed using MLR. As shown in Fig. 2c, untreated mDCs demonstrated the highest allogeneic T cell proliferation activity. However, the mDCs treated with EB demonstrated significantly lower dose-dependent levels of allogeneic T cell proliferation at the different DC to T cell ratios tested, suggesting that EB impaired the allogeneic T cell activating functions of mDCs and consequently suppressed the related immune responses.

EB Blocks the DC-Derived Th1-Polarizing and Th17-Polarizing Cytokines

DC-derived cytokines are required for the polarization of the adaptive immune response. Therefore, we investigated the potential effects of EB on the regulation of the expression of Th cell-polarizing cytokines. The DCs were pretreated with EB for 1 h and stimulated with LPS, and the steady-state levels of cytokine mRNAs were analyzed using quantitative PCR. As shown in Fig. 3, EB substantially inhibited the production of the inflammatory cytokine tumor necrosis factor-alpha (TNF-α), the Th1 cytokine IFN-γ, the Th1 cell-polarizing cytokine IL-12p35, and the Th17 cell-polarizing cytokines IL-6 and IL-12/23p40. However, IL-12p19 did not change significantly. We deduced that EB may have not influenced the subunit. These data suggest that EB suppressed the DC-mediated polarization of Th1 and Th17 cells and that it may be useful for the treatment of autoimmune inflammatory diseases that are mediated by Th1 and Th17 cells.

Overall, these in vitro studies demonstrated that EB significantly inhibited human $CD14^+$ monocyte-derived DC
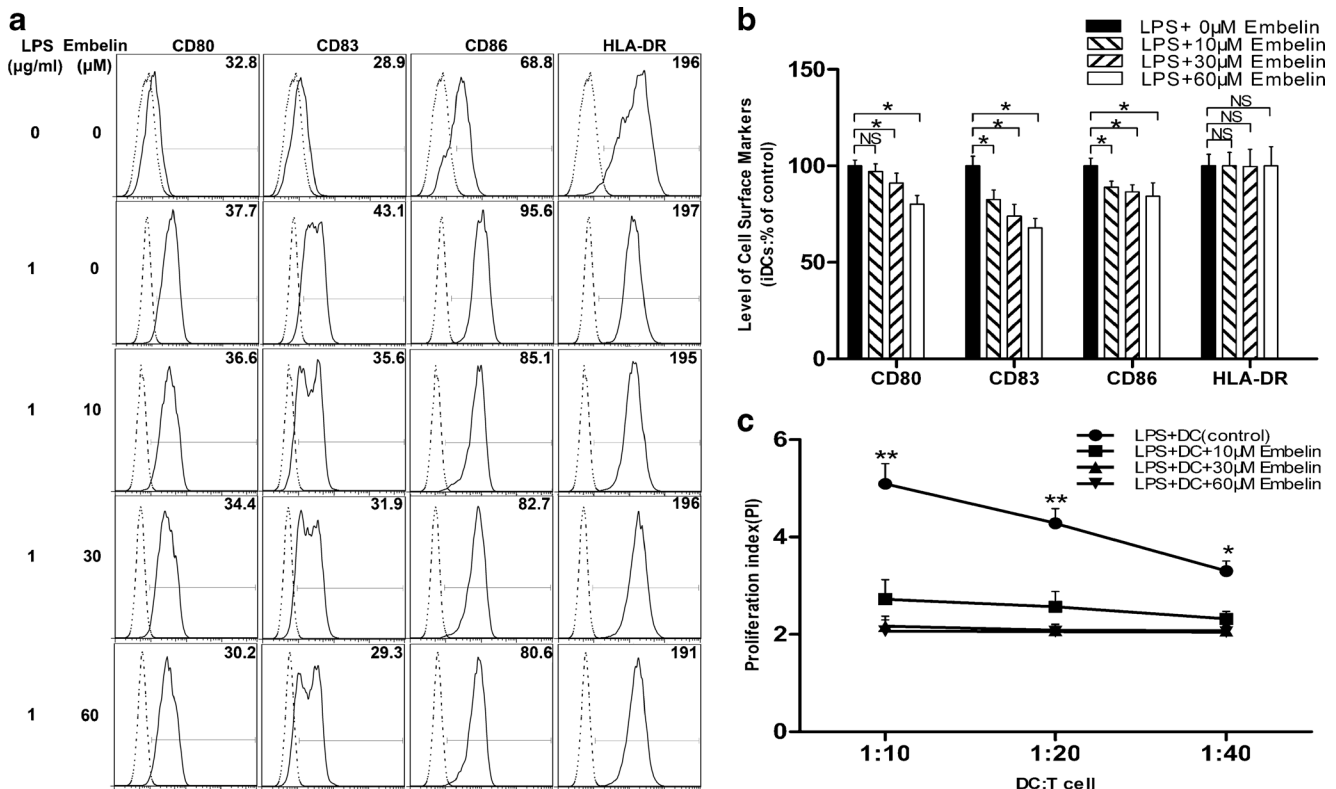
Fig. 2 EB suppressed iDCs maturation and mDC-induced allogeneic T cell proliferation. CD14^{+} monocytes were cultured in GM-CSF and IL-4 with or without different concentrations of EB. LPS (1 μg/ml) was added on day 5 in the presence of different doses of EB and cultured 2 days for DC maturation. Maturation of iDCs without the addition of EB and LPS was performed as a negative control. The FITC-conjugated DC surface markers CD80, CD83, CD86, and HLA-DR were used for staining. Flow cytometry analysis was performed on day 7. **a** Histograms of the cell surface marker staining from one of three independent experiments. The *numbers* indicate the MFI of the stained cells. **b** Relative levels of the markers compared to EB-untreated controls (100 %) from three independent experiments with means±SD. NS>0.05, *$p<0.05$ determined by Student's t test. **c** iDCs were treated with LPS on day 5 and were then treated with different concentrations of EB (10, 30, and 60 μM) for two more days. All mDCs were treated with mitomycin C, and all of the allogeneic CD4^{+} T cells were treated with CFSE. The mDCs were cocultured with the allogeneic CD4^{+} T cells at ratios of 1:10, 1:20, and 1:40 for 4 days. Flow cytometry analysis was performed to detect allogeneic T cell proliferation. The *y*-axis represents the PI. These data are representative of three independent experiments using different blood donors

differentiation and maturation, iDC antigen uptake ability, and antigen-presenting ability of mDCs. Specifically, EB suppressed the expression of co-stimulatory molecules, inflammatory cytokines, and Th1-polarizing and Th17-polarizing cytokines from DCs. These results suggest that EB exhibits anti-inflammatory and immunosuppressive properties.

EB Ameliorates the Clinical Severity of EAE in Mice

To investigate the functional anti-inflammatory and immunosuppressive roles of EB in vivo, the Th1/Th17 cell-mediated autoimmune inflammatory disease EAE was induced in C57BL/6 mice using the MOG$_{35-55}$ peptide. EB was administered intragastrically daily, and the mice were sacrificed on day 25 postimmunization. Compared with PBS-treated mice, the incidence of clinical symptoms in the 25 and 50 mg/kg/day EB-treated mice was reduced (Fig. 4a, b). In addition,

disease severity, assessed by the maximal and cumulative clinical scores, was significantly lower in EB-treated mice (Fig. 4c, d). These data suggest that EB significantly ameliorates the clinical outcome of EAE.

EB Limits CNS Inflammation and Demyelination

To characterize disease progression at the level of CNS injury, we performed a histological analysis of the lumbar spinal cord on day 15 postimmunization. At the peak of the acute phase of the disease, H&E staining demonstrated that the lumbar spinal cords from EB-treated mice exhibited smaller numbers of inflammatory cells in the white matter (Fig. 5a). The sections stained with Luxol fast blue revealed that PBS-treated mice exhibited large areas of demyelination; however, demyelination was markedly attenuated in EB-treated mice (Fig. 5b). Representative sections of lumbar spinal cords from PBS-

Fig. 3 EB affected the levels of Th1-inducing and Th17-inducing cytokine mRNA in DCs. iDCs at day 5 of culture were pretreated for 1 h with 30 μM EB and then stimulated with LPS. DCs were collected at 0, 1, 2, 4, 8, and 16 h, and the levels of the specified cytokine mRNAs were evaluated by quantitative PCR. Gene expression was routinely normalized based on GAPDH content. The data are representative of at least three independent experiments
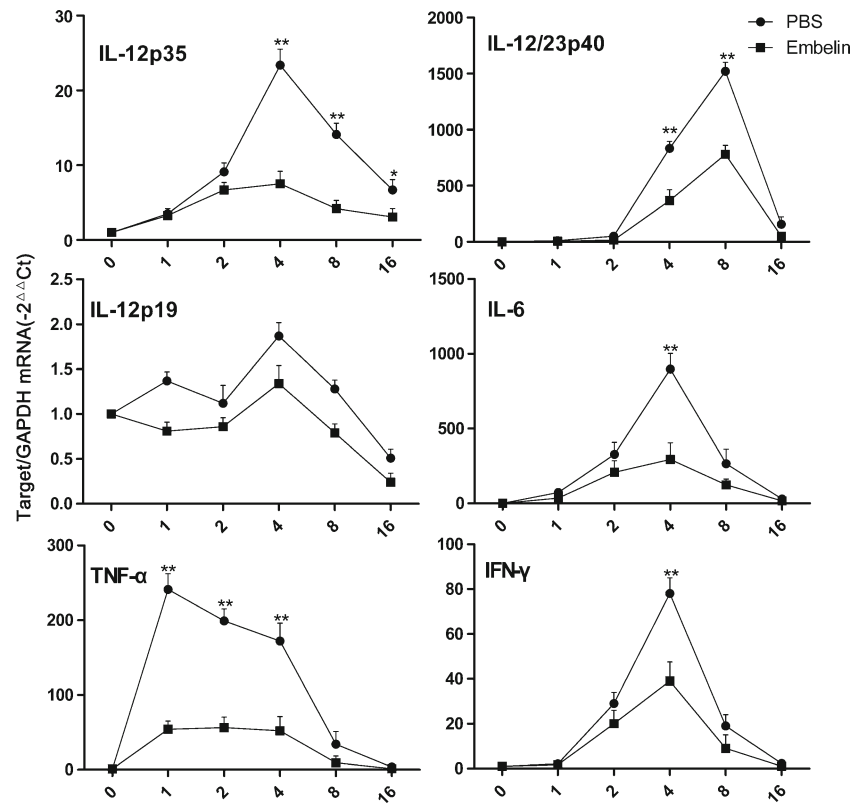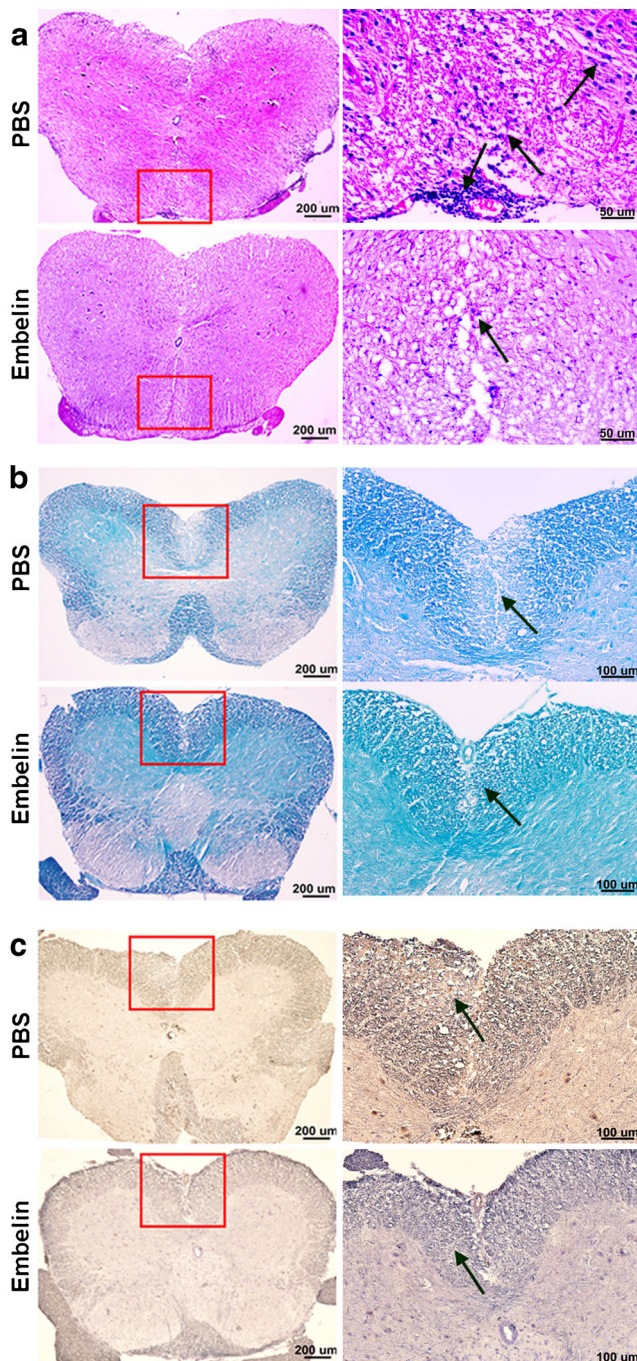

treated and EB-treated mice were immunostained using F4/80 (to stain macrophages and microglia), and the lumbar spinal cords from the EB-treated mice exhibited smaller numbers of

inflammatory cells in the CNS (Fig. 5c). In summary, EB inhibited CNS inflammation and demyelination in EAE, suggesting that EB improved the pathological symptoms of EAE.

Fig. 4 EB ameliorated the clinical severity of EAE in mice. EAE was induced in female C57BL/6 mice using MOG$_{35-55}$ and treated with EB as described in the "Materials and Methods" section. $n=12$ mice per group. The mean clinical score was the mean of the daily clinical scores observed from days 1 to 24 postimmunization. **a** For mice fed 25 mg/kg/day of EB (days 17–20, **$p<0.01$; days 21–24, *$p<0.05$). **b** For mice fed 50 mg/kg/day of EB (days 10–12, *$p<0.05$; days 16–24, **$p<0.01$). **c** The mean cumulative score was the mean of the sum of the daily clinical scores observed between days 1 and 24. **d** The mean maximum clinical score was calculated from the maximum clinical score of individual animals between days 1 and 24. The values represent the mean± SD. *$p<0.05$, **$p<0.01$ (Student's t test)
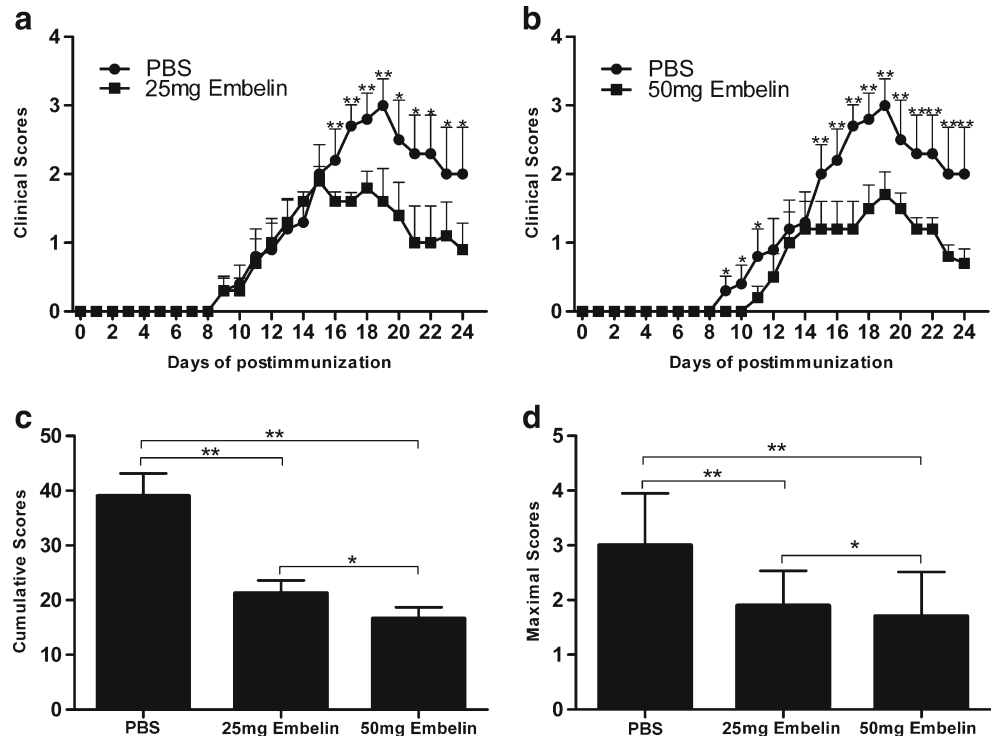
Fig. 5 Histopathological analysis of spinal cord sections from representative PBS-treated and EB-treated EAE mice. Serial sections of the spinal cord were obtained on day 17 after immunization. **a** H&E-stained section shows the infiltration of inflammatory cells in the white matter. The *arrows* indicate the inflammatory cells. **b** Luxol fast blue staining shows the areas of intact myelin (*blue*) and demyelination (*pink*). The *arrows* indicate the demyelination in the spinal cord, which includes sites associated with the infiltration of inflammatory cells, and indicate positive immunostaining. **c** Representative sections of lumbar spinal cords from PBS-treated and EB-treated mice immunostained for F4/80 (to stain macrophages and microglia). The *arrows* indicate positive immunostaining

EB Suppresses Th Cell Differentiation In Vivo

Because inflammatory Th1 and Th17 cells mediated autoimmune CNS inflammation and demyelination, we further investigated the impact of EB on the development of pathogenic Th1 and Th17 cell subsets in vitro and in vivo. In the ex vivo experiments, we examined the Th1 and Th17 cell subsets in splenocytes and the CNS through intracellular staining of IFN-γ and IL-17 cytokines. The data demonstrate that the percentage of IFN-γ-producing and IL-17-producing CD4$^+$ lymphocyte cells was lower in EB-treated mice compared with PBS-treated mice. These results indicate that EB suppression of EAE was concomitant with a reduction in the number of IFN-γ-producing Th1 cells and IL-17-producing Th17 cells (Fig. 6a, b). To examine inflammatory cytokine gene expression by infiltrating cells in the CNS during EAE, we analyzed the gene expression of IFN-γ, IL-17A, IL-4, IL-6, TNF-α, and TGF-β using quantitative real-time RT-PCR. The data reveal that IFN-γ and IL-17A expression was downregulated significantly, while IL-4 expression was significant upregulated. The expression of the cytokines IL-6, TNF-α, and TGF-β did not change significantly in EB-treated EAE mice (Fig. 7). These results indicate that inflammatory Th1 and Th17 cells were reduced in number, while Th2 cell numbers were increased by EB treatment.

EB Suppresses DCs in EAE Mice

In addition to the effects of EB on T cells, we investigated whether the regulatory effects of EB on the MOG-reactive T cell responses were attributable at least in part to the ability of the protein to alter the function of DCs. Splenocytes were obtained from EB-treated and PBS-treated EAE mice and were analyzed ex vivo for the expression of CD80, CD86, and MHC-II. As shown in Fig. 8, the surface expression of CD80, CD86, and MHC-II was reduced significantly in CD11c$^+$ cell populations from the EB-treated EAE mice compared with the PBS-treated mice. These data indicated that EB suppressed DCs in EAE mice in vivo.

Promotion of TGF-β/β-catenin and Inhibition of STAT3 Signaling in mDCs by EB

DCs were treated with LPS (1 μg/ml) overnight, and then treated with EB (30 μM) and lithium chloride (LiCl; 20 mM) for 30 min or 24 h. The treatment resulted in an increase in the levels of both TGF-β and β-catenin and a reduction in the levels of p-GSK-3β (Ser-9) and p-STAT3 (Tyr705) (Fig. 9a, b). The DCs were treated with 10, 30, and 60 μM of EB to detect the effect of EB on p-STAT3, β-catenin, TGF-β, and p-GSK-3β signaling by immunoblotting. Treatment with different doses of EB decreased the levels of the p-GSK-3β and p-STAT3 proteins and increased the levels of β-catenin and

Fig. 6 EB restricted T cell responses ex vivo. **a** Flow cytometry analysis of activation markers (IFN-γ and IL-17) on gated CD4$^+$ isolated from the spleens and CNS of PBS-treated and EB-treated EAE mice ($n=3$ mice per group) assessed on day 15 after the induction of EAE. Data are presented as a representative plot (**a**) and summary graph (**b**). For the flow cytometry Th1 and Th17 profile analyses, the cells were stimulated for 5 h with PMA/ionomycin and brefeldin and were stained for CD4, IFN-γ, and IL-17. Data are shown as the mean± SD representative of three mice per group. **p<0.01, ***p< 0.001 determined by Student's t test
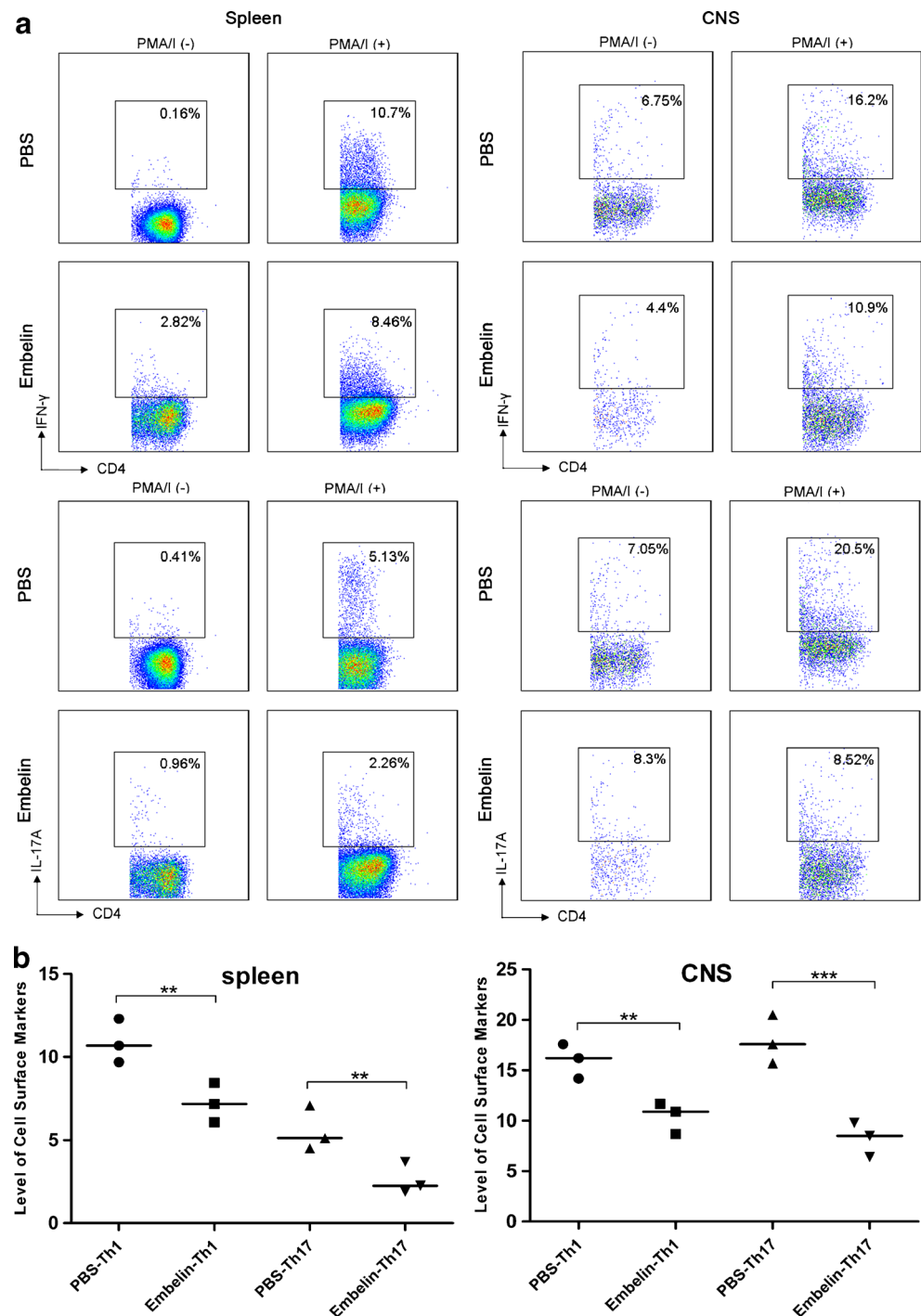

TGF-β in a dose-dependent manner after LPS stimulation (Fig. 9c, d).

Discussion

Although various molecular mechanisms have been described for the potent antitumor activities of EB, its potential effect on inflammatory and immune-mediated diseases such as MS and its animal model EAE remain unclear. In this study, we demonstrated that EB exhibits unique anti-inflammatory properties and has therapeutic potential for autoimmune inflammatory conditions. Our results demonstrate that EB can suppress human CD14$^+$ monocyte-derived DC differentiation and activation by decreasing the expression levels of several key DC surface markers, thereby inhibiting endocytosis in the cells and inhibiting the activation of mDCs and allogeneic T cell proliferation. Based on these studies, we further
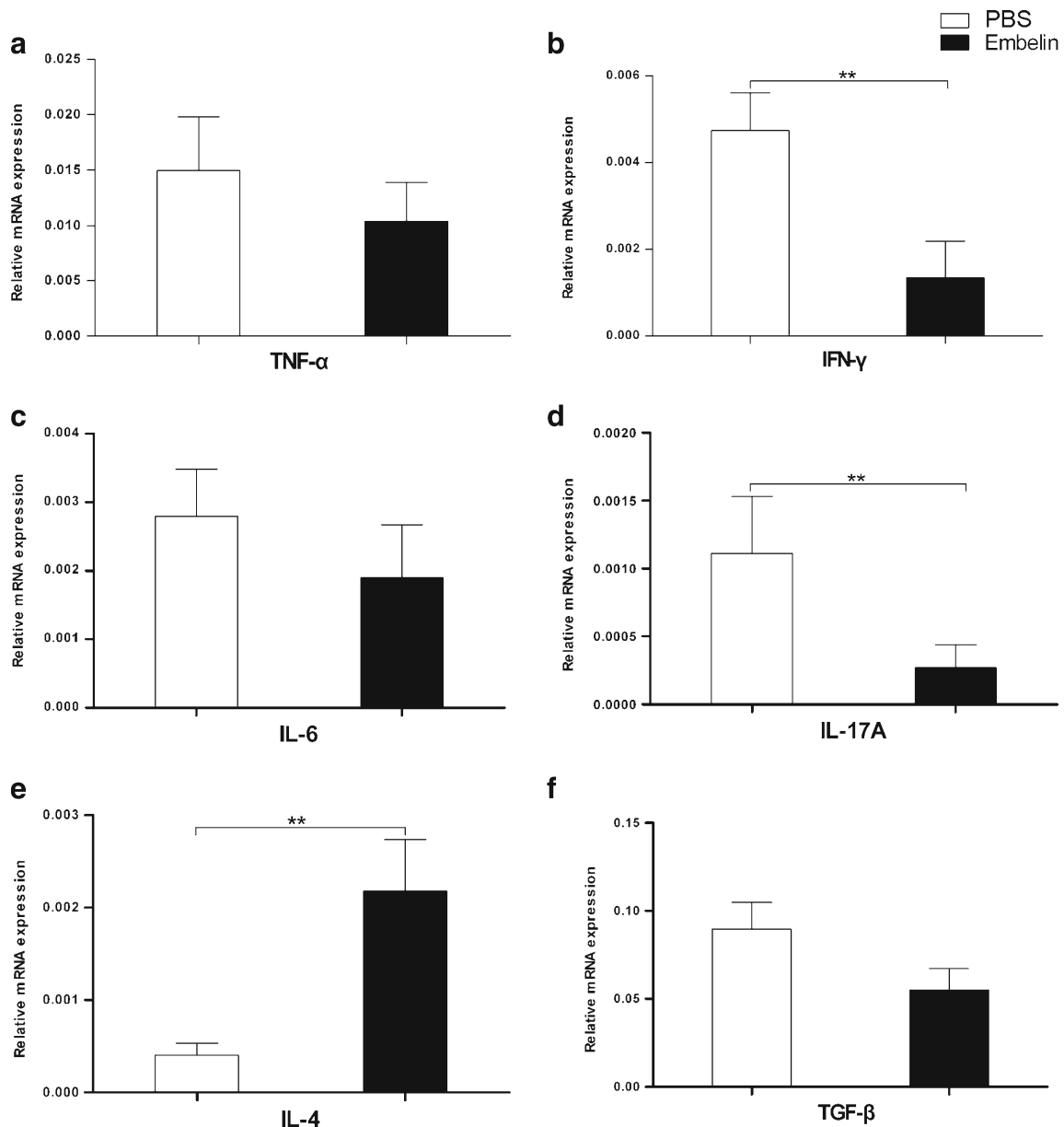
Fig. 7 EB inhibited inflammatory cytokine gene expression in infiltrating cells in the CNS during EAE. Mononuclear cells were separated from the brain and spinal cord of 50 mg/kg/day of EB-treated mice on day 15 using discontinuous 70 %/30 % Percoll gradients. The expression levels of IFN-γ, IL-17A, IL-4, IL-6, TNF-α, and TGF-β were evaluated using quantitative PCR. Gene expression was normalized to GAPDH expression levels. Data are shown as the mean±SD from at least three independent experiments

investigated the effect of EB in vivo. Our results demonstrate the efficacy of EB in ameliorating MS in the EAE animal model. Therefore, our results demonstrate that EB can affect human DC development, suggesting that EB could provide a therapeutic intervention for immune inflammatory diseases.

More importantly, the aim of this study was to elucidate the novel regulatory mechanism of EB and to probe the specific interactions of EB with molecular targets that are responsible for the effects of EB treatment on EAE. We reveal here the first major insight into the mechanism of EB, namely, that this compound inhibits DC function via TGF-β/β-catenin and STAT3 signaling, which leads to a reduction in the EAE clinical score and in CNS inflammation and demyelination. The novel finding of this study is that the anti-inflammatory effect of EB appears to require the presence of functional TGF-β/β-catenin and the absence of activated STAT3 in DCs. Consistent with previous studies by others [34, 35, 43], β-catenin signaling was found to program DCs into a tolerogenic state and limit the inflammatory response. TGF-β signaling in DCs is a prerequisite for the control of autoimmune encephalomyelitis.

We found that EB-induced inhibition of the differentiation of Th1 and Th17 cells was associated with a downregulation of the production of Th1-polarizing and Th17-polarizing

Fig. 8 EB suppressed CD11c^{+} DCs in vivo in EAE mice. **a** The splenocytes from 30 μM EB-treated or PBS-treated mice (*n*=3 mice per group) were stimulated with MOG$_{35-55}$ peptide and then stained for CD80, CD86, and MHC-II (*solid line*) or isotype control (*dashed line*) examination in the gated CD11c^{+} cell population. **b** Relative levels of the surface markers compared with the PBS-treated and EB-treated mice from three independent experiments with means±SD. **p*<0.05, ***p*<0.01 determined by Student's *t* test
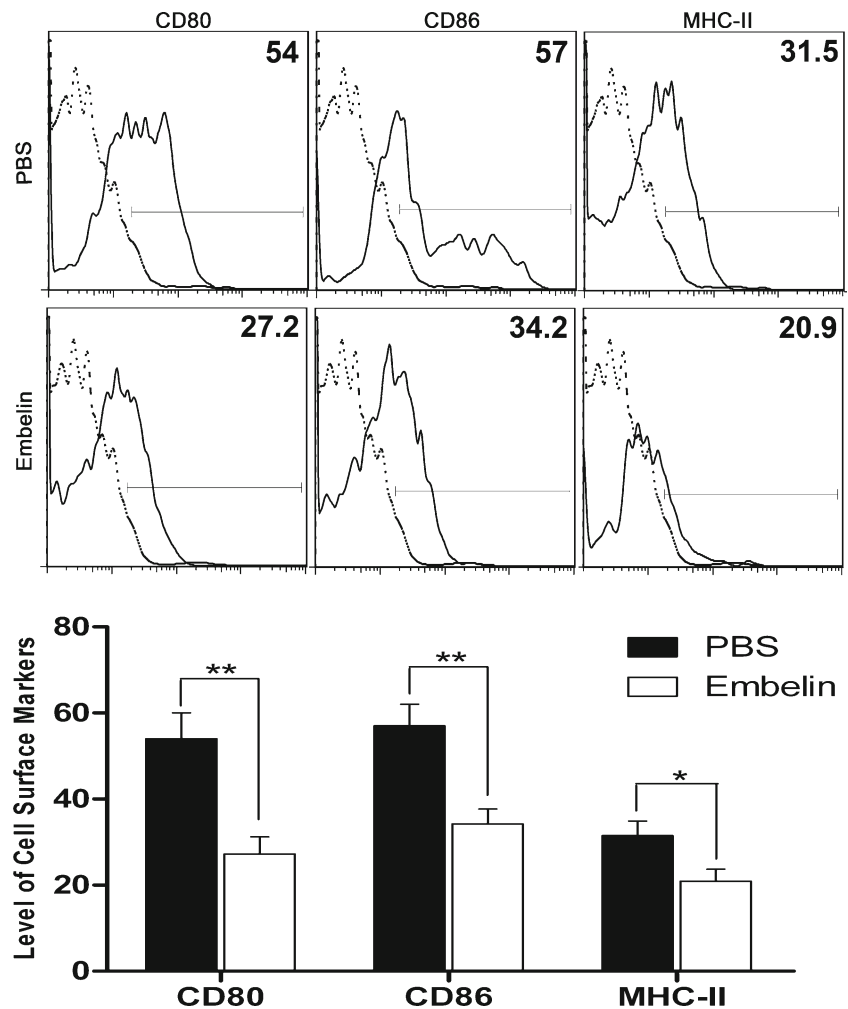
cytokines such as IL-12, IFN-γ, IL-6, and Il-23 in DCs. This is consistent with other studies that found that DCs with constitutively active β-catenin exhibited a diminished IL-12 response [34]. We also found that the expression of EB-induced cytokines, including IFN-γ (Th1), IL-17A (Th17), and IL-4 (Th2), changed significantly in cells infiltrating the CNS during EAE, but TGF-β cytokines did not change significantly. Treg cells secretion of cytokines including TGF-β, which may induce cell cycle arrest or apoptosis in effector T cells, and blocking co-stimulation and maturation of DCs [44–46].We infer that maybe only the Th1, Th2, and Th17 subsets were affected, not the Treg subsets. Similarly, Manicassamy et al. found that CD4^{+} T cells isolated from β-catenin$^{DC-/-}$ mice showed elevated expression of the Th17 cell-associated mRNAs IL-17, IL-21, and RORγt and the Th1 cell-associated mRNA IFN-γ when compared with CD4^{+} T cells isolated from β-catenin$^{fl/fl}$ mice [43].

Importantly, our results reveal, for the first time, that the anti-inflammatory effects of EB appear to be associated with increased β-catenin expression. Based on the important role of β-catenin in gut autoimmune disease [43], these findings

prompted us to investigate whether the anti-inflammatory effect of EB might be mediated by the activation of β-catenin. Treatment of DCs with LiCl, a potent inhibitor of GSK-3β and inducer of β-catenin signaling [47], resulted in a reduced level of GSK-3β and a corresponding increase in the β-catenin level (Fig. 9a). However, the level of TGF-β did not change in LiCl-treated DCs. LiCl suppresses astrogliogenesis from neural stem and progenitor cells by inhibiting the STAT3 pathway independently of GSK-3β [48]. We, therefore, reasoned that EB might suppress TGF-β and STAT3 independently, as was observed with LiCl. This was consistent with previous studies that found that EB is a potent inhibitor of STAT3 [29]. LiCl has been found to inhibit EAE development in rats [49]. The STAT3 signaling pathway regulates β-catenin and GSK-3β protein expression in hepatocellular carcinoma [50]. Our results indicated that EB might prevent the development of EAE through TGF-β/β-catenin and STAT3 signaling collectively (Fig. 8a). We also found that the GSK-3β level was reduced in DCs. Our conclusion was further supported by the finding that the level of GSK-3β was highly upregulated during Th17 polarization, which is particularly
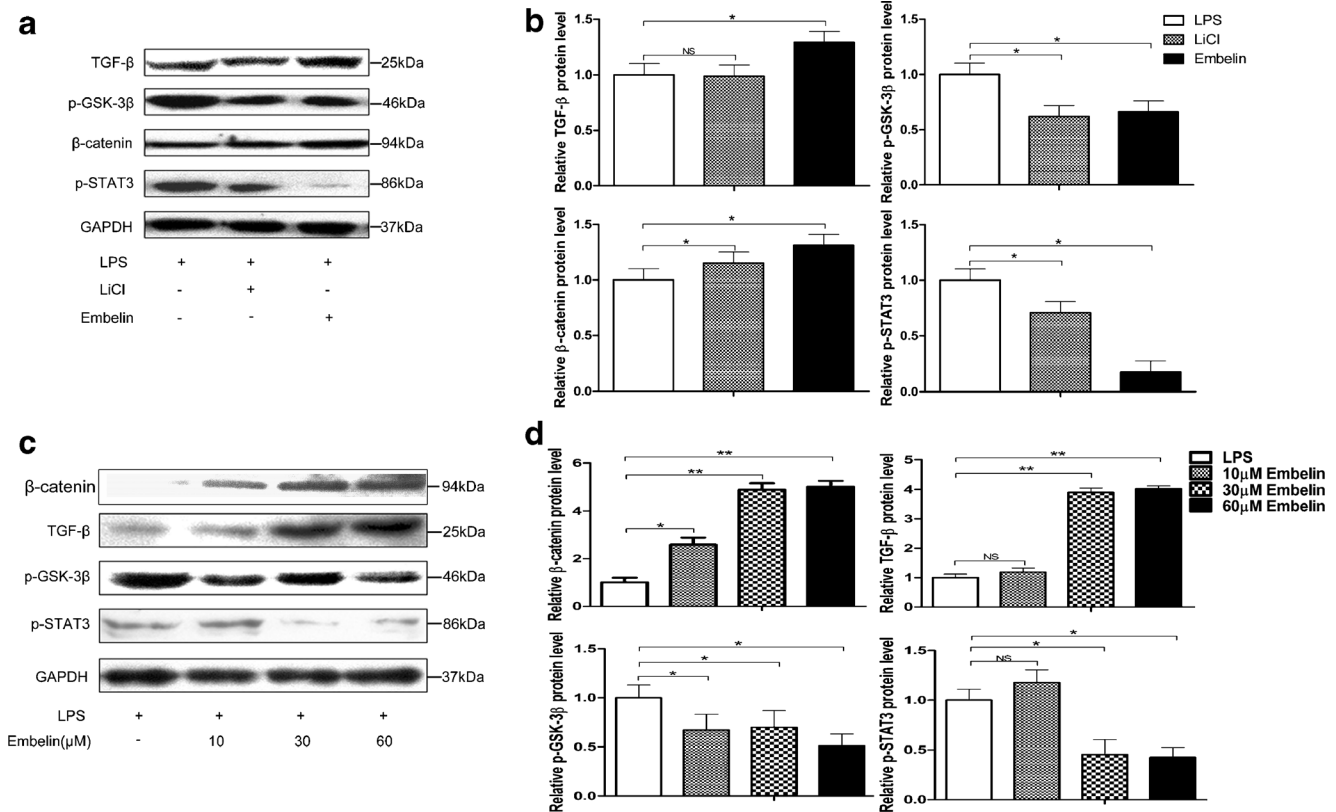
Fig. 9 EB promotes TGF-β/β-catenin and inhibits STAT3 signaling in mDCs. **a** DCs were treated with LPS (1 μg/ml) overnight, and then treated with EB (30 μM) and LiCl (20 mM) for either 30 min or 24 h to investigate the effect on p-STAT3, TGF-β, β-catenin, and p-GSK-3β signaling (diluted 1:1,000). **c** DCs were treated with 10, 30, and 60 μM EB to investigate its effect on p-STAT3, TGF-β, β-catenin, and p-GSK-3β signaling (diluted 1:1,000). The experiment was performed independently in triplicate and one representative image is shown. The protein bands were quantified using ImageJ and are presented as a fold of the control (**b**, **d**). Data are shown as the mean±SD based on three independent experiments. NS>0.05, *$p<0.05$, **$p<0.01$ determined by Student's t test

notable considering that GSK-3β levels are generally very stable in numerous cell types and conditions [51].

With regard to the regulatory mechanism and molecular targets of EB, we presented evidence showing that the effect of EB treatment was associated primarily with the selective inhibition of DC functions through the TGF-β/β-catenin and STAT3 pathway. Mechanistically, EB acted through the TGF-β/β-catenin and STAT3 pathway, which was activated independently of externally introduced cytokines. In this study, we demonstrated that EB affected LPS-induced DC maturation and induced a general inhibition of cytokine production, suggesting that EB could serve as a potent anti-inflammatory drug in a number of inflammatory diseases.

In summary, we demonstrated that EB, a novel XIAP inhibitor, significantly increased TGF-β/β-catenin signaling and decreased STAT3 phosphorylation in DCs. These conditions are critical for maintaining DCs in their tolerogenic state via a reduction in the expression of pro-inflammatory factors such as IFN-γ, IL-12, IL-6, and IL-23. EB treatment of DCs inhibited their production of Th1-polarizing and Th17-polarizing cytokines, maybe indirectly influencing Th cell differentiation. In vivo, EB treatment inhibited mDC and Th cell differentiation, which further led to a reduction in the EAE clinical score and in CNS inflammation and demyelination. Therefore, these data suggest that EB inhibition can be exploited as a therapeutic strategy to control pathological conditions, such as autoimmune diseases, that are induced by the functional expansion of Th1 and Th17 cells.

References

1. Gupta OP, Ali MM, Ray Ghatak BJ, Atal CK (1977) Some pharmacological investigations of embelin and its semisynthetic derivatives. Indian J Physiol Pharmacol 21:31–39
2. Chitra M, Sukumar E, Devi CS (1995) [3H]-thymidine uptake and

lipid peroxidation by tumor cells on embelin treatment: an in vitro study. Oncology 52:66–68

3. Nikolovska-Coleska Z, Xu L, Hu Z, Tomita Y, Li P, Roller PP, Wang R, Fang X, Guo R, Zhang M, Lippman ME, Yang D, Wang S (2004) Discovery of embelin as a cell-permeable, small-molecular weight inhibitor of XIAP through structure-based computational screening of a traditional herbal medicine three-dimensional structure database. J Med Chem 47:2430–2440

4. Ahn KS, Sethi G, Aggarwal BB (2007) Embelin, an inhibitor of X chromosome-linked inhibitor-of-apoptosis protein, blocks nuclear factor-kappaB (NF-kappaB) signaling pathway leading to suppression of NF-kappaB-regulated antiapoptotic and metastatic gene products. Mol Pharmacol 71:209–219

5. Sasaki Y, Minamizawa M, Ambo A, Sugawara S, Ogawa Y, Nitta K (2008) Cell-penetrating peptide-conjugated XIAP-inhibitory cyclic hexapeptides enter into Jurkat cells and inhibit cell proliferation. Febs J 275:6011–6021

6. Mori T, Doi R, Kida A, Nagai K, Kami K, Ito D, Toyoda E, Kawaguchi Y, Uemoto S (2007) Effect of the XIAP inhibitor embelin on TRAIL-induced apoptosis of pancreatic cancer cells. J Surg Res 142:281–286

7. Mareninova OA, Sung KF, Hong P, Lugea A, Pandol SJ, Gukovsky I, Gukovskaya AS (2006) Cell death in pancreatitis: caspases protect from necrotizing pancreatitis. J Biol Chem 281:3370–3381

8. Aird KM, Ding X, Baras A, Wei J, Morse MA, Clay T, Lyerly HK, Devi GR (2008) Trastuzumab signaling in ErbB2-overexpressing inflammatory breast cancer correlates with X-linked inhibitor of apoptosis protein expression. Mol Cancer Ther 7:38–47

9. Dai Y, Qiao L, Chan KW, Yang M, Ye J, Ma J, Zou B, Gu Q, Wang J, Pang R, Lan HY, Wong BC (2009) Peroxisome proliferator-activated receptor-gamma contributes to the inhibitory effects of embelin on colon carcinogenesis. Cancer Res 69:4776–4783

10. Heo JY, Kim HJ, Kim SM, Park KR, Park SY, Kim SW, Nam D, Jang HJ, Lee SG, Ahn KS, Kim SH, Shim BS, Choi SH (2011) Embelin suppresses STAT3 signaling, proliferation, and survival of multiple myeloma via the protein tyrosine phosphatase PTEN. Cancer Lett 308:71–80

11. Dai Y, Desano J, Qu Y, Tang W, Meng Y, Lawrence TS, Xu L (2011) Natural IAP inhibitor embelin enhances therapeutic efficacy of ionizing radiation in prostate cancer. Am J Cancer Res 1:128–143

12. Xu M, Cui J, Fu H, Proksch P, Lin W, Li M (2005) Embelin derivatives and their anticancer activity through microtubule disassembly. Planta Med 71:944–948

13. Kim SW, Kim SM, Bae H, Nam D, Lee JH, Lee SG, Shim BS, Kim SH, Ahn KS, Choi SH, Sethi G, Ahn KS (2013) Embelin inhibits growth and induces apoptosis through the suppression of Akt/mTOR/ S6K1 signaling cascades. Prostate 73(3):296–305

14. Gandhi GR, Stalin A, Balakrishna K, Ignacimuthu S, Paulraj MG, Vishal R (2013) Insulin sensitization via partial agonism of PPARγ and glucose uptake through translocation and activation of GLUT4 in PI3K/p-Akt signaling pathway by embelin in type 2 diabetic rats. Biochim Biophys Acta 1830(1):2243–2255

15. Banchereau J, Steinman RM (1998) Dendritic cells and the control of immunity. Nature 392:245–252

16. Pulendran B (2004) Modulating vaccine responses with dendritic cells and Toll-like receptors. Immunol Rev 199:227–250

17. Steinman RM, Hawiger D, Nussenzweig MC (2003) Tolerogenic dendritic cells. Annu Rev Immunol 21:685–711

18. Mellman I, Steinman RM (2001) Dendritic cells: specialized and regulated antigen processing machines. Cell 106:255–258

19. Trombetta ES, Mellman I (2005) Cell biology of antigen processing in vitro and in vivo. Annu Rev Immunol 23:975–1028

20. Engelhardt B (2008) Immune cell entry into the central nervous system: involvement of adhesion molecules and chemokines. J Neurol Sci 274:23–26

21. Goverman J (2009) Autoimmune T cell responses in the central nervous system. Nat Rev Immunol 9:393–407

22. Hamann I, Zipp F, Infante-Duarte C (2008) Therapeutic targeting of chemokine signaling in multiple sclerosis. J Neurol Sci 274: 31–38

23. Cua DJ, Hinton DR, Stohlman SA (1995) Self-antigen-induced Th2 responses in experimental allergic encephalomyelitis (EAE)-resistant mice. Th2-mediated suppression of autoimmune disease. J Immunol 155(8):4052–4059

24. Krishnamoorthy G, Wekerle H (2009) EAE: an immunologist's magic eye. Eur J Immunol 39:2031–2035

25. Bai XF, Shi FD, Xiao BG, Li HL, van der Meide PH, Link H (1997) Nasal administration of myelin basic protein prevents relapsing experimental autoimmune encephalomyelitis in DA rats by activating regulatory cells expressing IL-4 and TGF-beta mRNA. J Neuroimmunol 80(1–2):65–75

26. Johns LD, Flanders KC, Ranges GE, Sriram S (1991) Successful treatment of experimental allergic encephalomyelitis with transforming growth factor-β1. J Immunol 147:1792–1796

27. Racke MK, Dhib-Jalbut S, Cannella B, Albert PS, Raine CS, McFarlin DE (1991) Prevention and treatment of chronic relapsing experimental allergic encephalomyelitis by transforming growth factor-beta 1. J Immunol 146(9):3012–3017

28. Racke MK, Cannella B, Albert P, Sporn M, Raine CS, McFarlin DE (1992) Evidence of endogenous regulatory function of transforming growth factor-beta 1 in experimental allergic encephalomyelitis. Int Immunol 4(5):615–620

29. Kuruvilla AP, Shah R, Hochwald GM, Liggitt HD, Palladino MA, Thorbecke GJ (1991) Protective effect of transforming growth factor beta 1 on experimental autoimmune diseases in mice. Proc Natl Acad Sci U S A 88(7):2918–2921

30. Johns LD, Sriram S (1993) Experimental allergic encephalomyelitis: neutralizing antibody to TGF beta 1 enhances the clinical severity of the disease. J Neuroimmunol 47(1):1–7

31. Issazadeh S, Mustafa M, Ljungdahl A, Höjeberg B, Dagerlind A, Elde R, Olsson T (1995) Interferon gamma, interleukin 4 and transforming growth factor beta in experimental autoimmune encephalomyelitis in Lewis rats: dynamics of cellular mRNA expression in the central nervous system and lymphoid cells. J Neurosci Res 40(5):579–590

32. Kinzler KW, Vogelstein B (1996) Lessons from hereditary colorectal cancer. Cell 87:159–170

33. Laouar Y, Town T, Jeng D, Tran E, Wan Y, Kuchroo VK, Flavell RA (2008) TGF-beta signaling in dendritic cells is a prerequisite for the control of autoimmune encephalomyelitis. Proc Natl Acad Sci U S A 105(31):10865–10870

34. Fu C, Jiang A (2010) Generation of tolerogenic dendritic cells via the E-cadherin/beta-catenin-signaling pathway. Immunol Res 46:72–78

35. Ding Y, Shen S, Lino AC, Curotto de Lafaille MA, Lafaille JJ (2008) Beta-catenin stabilization extends regulatory T cell survival and induces anergy in nonregulatory T cells. Nat Med 14(2):162–169

36. Valenta T, Hausmann G, Basler K (2012) The many faces and functions of β-catenin. EMBO J 31(12):2714–2736

37. Logan CY, Nusse R (2004) The Wnt signaling pathway in development and disease. Annu Rev Cell Dev Biol 20:781–810

38. Christodoulides C, Lagathu C, Sethi JK, Vidal-Puig A (2009) Adipogenesis and WNT signalling. Trends Endocrinol Metab 20: 16–24

39. Liu C, Li Y, Semenov M, Han C, Baeg GH, Tan Y, Zhang Z, Lin X, He X (2002) Control of beta-catenin phosphorylation/degradation by a dual-kinase mechanism. Cell 108:837–847

40. Vander Lugt B, Beck ZT, Fuhlbrigge RC, Hacohen N, Campbell JJ, Boes M (2011) TGF-β suppresses β-catenin-dependent tolerogenic activation program in dendritic cells. PLoS One 6(5):e20099

41. Loma I, Heyman R (2011) Multiple sclerosis: pathogenesis and treatment. Curr Neuropharmacol 9(3):409–416

42. Stromnes IM, Governan JM (2006) Active induction of experimental allergic encephalomyelitis. Nat Protoc 1(4):1810–1819

43. Manicassamy S, Reizis B, Ravindran R, Nakaya H, Salazar-Gonzalez RM, Wang YC, Pulendran B (2010) Activation of beta-catenin in dendritic cells regulates immunity versus tolerance in the intestine. Science 329(5993):849–853

44. Takahashi T, Kuniyasu Y, Toda M, Sakaguchi N, Itoh M, Iwata M, Shimizu J, Sakaguchi S (1998) Immunologic self-tolerance maintained by CD25$^+$CD4$^+$ naturally anergic and suppressive T cells: induction of autoimmune disease by breaking their anergic/suppressive state. Int Immunol 10(12):1969–1980

45. Shevach EM (2000) Regulatory T cells in autoimmunity. Annu Rev Immunol 18:423–449

46. Curotto de Lafaille MA, Lafaille JJ (2009) Natural and adaptive foxp3$^+$ regulatory T cells: more of the same or a division of labor? Immunity 30(5):626–635

47. Stambolic V, Ruel L, Woodgett JR (1996) Lithium inhibits glycogen synthase kinase-3 activity and mimics wingless signalling in intact cells. Curr Biol 6:1664–1668

48. Levine S, Saltzman A (1991) Inhibition of experimental allergic encephalomyelitis by lithium chloride: specific effect or nonspecific stress? Immunopharmacology 22(3):207–213

49. Zhu Z, Kremer P, Tadmori I, Ren Y, Sun D, He X, Young W (2011) Lithium suppresses astrogliogenesis by neural stem and progenitor cells by inhibiting STAT3 pathway independently of glycogen synthase kinase 3 beta. PLoS One 6(9):e23341

50. Wang XH, Meng XW, Xing H, Qu B, Han MZ, Chen J, Fan YJ, Lu CQ, Lu ZW (2011) STAT3 and beta-catenin signaling pathway may affect GSK-3beta expression in hepatocellular carcinoma. Hepato gastroenterology 58(106):487–491

51. Jope RS, Johnson GV (2004) The glamour and gloom of glycogen synthase kinase-3. Trends Biochem Sci 29(2):95–102